



Published in final edited form as:

Gastroenterology. 2022 November ; 163(5): 1334–1350.e14. doi:10.1053/j.gastro.2022.07.016.

SMAD4 suppresses colitis-associated carcinoma through inhibition of CCL20/CCR6-mediated inflammation

David N. Hanna^{1,*}, Paula Marincola Smith^{1,2,*}, Sergey V. Novitskiy³, M. Kay Washington^{4,5}, Jinghuan Zi¹, Connie J. Weaver¹, Jalal A. Hamaamen¹, Keeli B. Lewis¹, Jing Zhu¹, Jing Yang^{2,6}, Qi Liu⁶, R. Daniel Beauchamp^{1,2,4,7,8,#}, Anna L. Means^{1,2,4,7,8,#}

¹Department of Surgery, Section of Surgical Sciences, Vanderbilt University Medical Center, Nashville, TN

²Graduate Program in Cancer Biology, Vanderbilt University School of Medicine, Nashville, TN

³Department of Medicine, Vanderbilt University Medical Center, Nashville, Tennessee

⁴Vanderbilt-Ingram Cancer Center, Vanderbilt University Medical Center, Nashville, Tennessee

⁵Department of Pathology, Microbiology, and Immunology, Vanderbilt University Medical Center, Nashville, Tennessee

⁶Department of Biostatistics, Vanderbilt University Medical Center, Nashville, TN

⁷Digestive Disease Research Center, Vanderbilt University Medical Center, Nashville, TN

⁸Department of Cell and Developmental Biology, Vanderbilt University School of Medicine, Nashville, TN, USA

Corresponding Authors: R. Daniel Beauchamp, MD, FACS, Medical Center North, D-2300, 1161 21st Ave South, Nashville, TN 37232, Daniel.beauchamp@vumc.org, Telephone: 615-322-2363, Fax: 615-343-5365; Anna L. Means, PhD, Medical Center North, D-2307, 1161 21st Ave South Nashville, TN 37232, Anna.means@vumc.org, Telephone: 615-343-0922, Fax: 615-343-8119.

*David N. Hanna and Paula Marincola Smith share co-first authorship

#R. Daniel Beauchamp and Anna L. Means are co-corresponding authors

Author Contributions:

- DNH – conceptualization, data curation, formal analysis, investigation, methodology, visualization, writing – original draft, writing – review and editing
- PMS: conceptualization, data curation, funding acquisition, investigation, methodology, visualization, writing – original draft
- SVN – methodology, resources, supervision, software, validation, writing – reviewing and editing
- MKW – formal analysis, investigation, resources, validation, writing – reviewing and editing
- JZ, CJW, JAH, KBL – data curation, investigation, writing – reviewing and editing
- JZ, JY, QL – data curation, formal analysis, investigation, methodology, writing – review and editing
- RDB – conceptualization, funding acquisition, methodology, project administration, resources, supervision, validation, writing – review and editing
- ALM – conceptualization, funding acquisition, methodology, project administration, resources, supervision, writing – review and editing

Publisher's Disclaimer: This is a PDF file of an unedited manuscript that has been accepted for publication. As a service to our customers we are providing this early version of the manuscript. The manuscript will undergo copyediting, typesetting, and review of the resulting proof before it is published in its final form. Please note that during the production process errors may be discovered which could affect the content, and all legal disclaimers that apply to the journal pertain.

Disclosures: The authors have declared that no conflict of interest exists.

Transcript Profiling: RNA sequencing data files are publicly available on the National Institute of Health Gene Expression Omnibus (GEO) database accession number GSE189667

Writing Assistance: None

Data Transparency Statement: All data, analytic methods, and study materials will be made available to researchers upon request.

Abstract

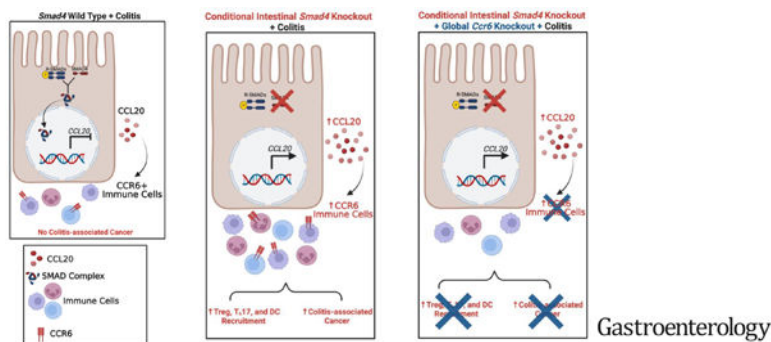
Background & Aims: We previously reported that colon epithelial cell silencing of *Smad4* increased epithelial expression of inflammatory genes, including the chemokine CCL20, and increased susceptibility to colitis-associated cancer. Here, we examine the role of the chemokine/receptor pair CCL20/CCR6 in mediating colitis-associated colon carcinogenesis induced by SMAD4 loss.

Methods: *In silico* analysis of *SMAD4*, *CCL20*, and *CCR6* mRNA expression was performed on published transcriptomic data from human ulcerative colitis (UC), and colon and rectal cancer samples. Immunohistochemistry for CCL20 and CCR6 was performed on human tissue microarrays (TMAs) comprising human UC-associated cancer specimens. Mice with conditional, epithelial-specific *Smad4* loss with and without germline deletion of the *Ccr6* gene were subjected to colitis and followed for up to 3 months. Tumors were quantified histologically, and immune cell populations were analyzed by flow cytometry and immunostaining.

Results: In human UC-associated cancers, loss of epithelial SMAD4 was associated with increased CCL20 expression and CCR6+ cells. SMAD4 loss in mouse colon epithelium led to enlarged gut-associated lymphoid tissues and recruitment of immune cells to the mouse colon epithelium and stroma, particularly Treg, T_H17, and dendritic cells. Loss of CCR6 abrogated these immune responses and significantly reduced the incidence of colitis-associated tumors observed with loss of SMAD4 alone.

Conclusions: Regulation of mucosal inflammation is central to SMAD4 tumor suppressor function in the colon. A key downstream node in this regulation is suppression of epithelial CCL20 signaling to CCR6 in immune cells. Loss of SMAD4 in the colon epithelium increases CCL20 expression and chemoattraction of CCR6+ immune cells, contributing to greater susceptibility to colon cancer.

Graphical Abstract



Lay Summary

The SMAD4 tumor suppressor gene regulates communication between colon cells and surrounding immune cells. In the setting of colitis, SMAD4 loss leads to increased immune cells and promote tumor development.

Keywords

Inflammatory bowel disease; colorectal cancer; SMAD4; inflammation

Introduction

Chronic inflammation is a predisposing factor for many cancers, including colorectal cancer (CRC), which is the third most common cancer worldwide^{1, 2}. Inflammatory bowel disease (IBD) patients exemplify this relationship, as they demonstrate a markedly elevated risk of developing CRC, often early in life³.

Transforming growth factor β (TGF β) family signaling functions in a critical tumor suppressor role, particularly within the alimentary tract. In the canonical pathway, TGF β signaling is dependent on SMAD4 as the pathway's common mediator⁴. Previous work from our lab demonstrated that TGF β signaling via SMAD4 blocks or represses the effects of pro-inflammatory cytokines in colonic epithelium⁵. Additionally, we found that conditional knockout of the *Smad4* gene in murine intestinal epithelial cells led to a striking increase in epithelial inflammatory signaling, stromal leukocyte infiltration, and profoundly increased susceptibility to colitis-associated cancer (CAC) development compared to SMAD4+ control mice⁵.

We previously identified that expression of C-C motif chemokine ligand 20 (CCL20) is markedly increased in colon epithelial cells *in vivo* and *in vitro* after loss of SMAD4 or inhibition of TGF β receptors⁵. CCL20 acts via its sole receptor, C-C motif chemokine receptor 6 (CCR6), and is expressed on multiple immune cell subtypes including T_H17 cells, Tregs, B cells, multiple dendritic cell (DC) subsets, and others^{6, 7}. In humans, CCL20 is upregulated in both ulcerative colitis and Crohn's disease, and is elevated in sporadic colorectal adenomas and in CRC, suggesting that it may influence cancer susceptibility⁸⁻¹⁰.

Here we demonstrate that *SMAD4* mRNA expression is negatively correlated with *CCL20* and *CCR6* mRNA expression in human IBD specimens, loss of SMAD4 expression is associated with increased CCL20 expression and CCR6+ cells in human ulcerative colitis-associated colon cancer specimens, and ulcerative colitis-associated cancers with SMAD4 loss have increased immune cell infiltration. Furthermore, we found that conditional colon epithelial cell *Smad4* gene loss in mice leads to increased expression of inflammation-related genes within the colonic sub-epithelial stromal tissues, including *Ccr6*, and an increase in gut-associated lymphoid tissue (GALT) area that accompanies the increase in colonocyte expression of *Ccl20*. Following dextran sodium sulfate (DSS) -induced colitis, specific immune populations were increased by SMAD4 loss, including stromal Tregs and stromal and epithelial-associated CD4+ IL17a+ T cells (T_H17) and DC subtypes. Notably, these cells are all known to be regulated by CCR6 activity and loss of *Ccr6* abrogated much of the phenotype that was induced by epithelial *Smad4* loss alone. Furthermore, we demonstrate that CAC development due to epithelial SMAD4 loss is dependent on an intact CCL20/CCR6 axis.

Materials and Methods

In silico Analysis of Microarray Data and The Cancer Genome Atlas (TCGA)

Gene expression in IBD patients and healthy controls was analyzed from published transcriptomic data generated from endoscopic biopsy samples and analyzed by Microarray (GSE75214)¹¹ as we have previously published¹². To determine the relationship between *SMAD4*, *CCL20*, and *CCR6* expression in sporadic colon cancer specimens, rectal cancer specimens, and healthy representative controls, the TCGA database (<https://www.cancer.gov/tcga>) was analyzed utilizing the Firehose web browser from the Broad Institute (<https://gdac.broadinstitute.org/>).

Immunohistochemical staining and Multiplex Immunofluorescent (mxIF) of Human Tissues

Tissue microarrays (TMAs) were created from 34 ulcerative colitis-associated cancer (UCAC) specimens, 18 UC-associated dysplasia specimens, 34 UC specimens uninvolved with cancer, and 5 healthy control specimens (HCc). For quantification of CCR6+ cells within the stroma, CCR6+ cell counts were normalized to total stromal area. GALTs were excluded from the total stromal area as they primarily consist of immune cells and many samples did not have GALTs. For evaluation of CCL20 expression, a collaborating pathologist (MKW) scored the samples for staining intensity and percentage of epithelium involved with CCL20 staining blinded to SMAD4 status. If multiple cores existed for a particular sample, the mean cell count, staining intensity, or percent positivity was used. SMAD4 expression was determined by immunohistochemistry (rabbit anti-SMAD ab40759 Abcam; Waltham, MA). SMAD4 negative samples were defined as those with no SMAD4 expression in the nucleus or cytoplasm, while samples with SMAD4 detected in the cytoplasm but not the nucleus were classified as cytoplasm positive. Samples with SMAD4 detected in both the nucleus and cytoplasm were labeled as nuclear positive.

For MxIF, another TMA was previously created from de-identified UCACs and SMAD4 status was previously determined by immunohistochemistry⁵. Sequential staining (Supplementary Table S1), single-cell segmentation, and cell quantification was performed by the Vanderbilt University Medical Center (VUMC) Digital Histology Shared Resource.

Mouse Model

Animal work was performed with approval from the Vanderbilt University Institutional Animal Care and Use Committee and followed ARRIVE guidelines. We previously published that tamoxifen-treated *Lrig1^{CreERT}Smad4^{fl/fl}* (termed *Smad4^{Lrig1}*) mice have greater than 90% loss of SMAD4 in their colon epithelium, thus creating tissue-specific inducible loss of *Smad4*⁵. SMAD4-expressing control mice (*Smad4^{fl/fl}* mice with no Cre alleles) treated with tamoxifen are referred to as SMAD4+ or control mice.

For animal experiments involving mice with or without *Ccr6* expression, mice with *Lrig1^{CreERT2}* and *Smad4^{fl/fl}* alleles were bred with mice from Jackson Laboratory (Bar Harbor, ME) that have *GFP* knocked into the *Ccr6* coding region such that cells transcribing from the *Ccr6* promoter can be tracked by GFP protein expression in heterozygous *Ccr6^{GFP/+}* mice and in *Ccr6^{GFP/GFP}* null mice¹³.

Experimental colitis was induced using 2% DSS (MP Biomedicals, Santa Ana, CA) in drinking water for 5 days, followed by 5 days of recovery, in 3 consecutive cycles. Controls were sibling littermates and cage mates. After tamoxifen treatment, bedding was mixed among cages within an experiment once per week.

RNA-Sequencing

For bulk RNAseq, three *Smad4^{Lrig1}* and three SMAD4+ control mice were dissected one month after administration of tamoxifen. Colons were stripped of crypts as published⁵. Stroma was scraped from underlying muscle for RNA extraction and RNAseq was performed by the Vanderbilt Technologies for Advanced Genomics (VANTAGE) core facility. The data files are publicly available on the National Institute of Health Gene Expression Omnibus database (GSE189667)^{14, 15}. Additional detail is provided in Supplementary Methods.

RNAScope® In Situ Hybridization

In situ hybridization by RNAScope® technique was performed according to the manufacturer's instructions on 5µm thick sections from five *Smad4^{Lrig1}* and five SMAD4+ control mice [Advanced Cell Diagnostics (ACD), Newark, CA, USA]. To quantify differential *Ccl20* expression, specific colorimetric dots corresponding with mRNA copies were counted in each positive cell. To quantify cells expressing *Ccr6*, the number of positive cells were counted among the distalmost 100 crypts.

Mouse Histology and Immunostaining

Mouse tissues were processed as described¹⁶. For analysis of GALTs, three 5µm sections were cut and examined per mouse, each 1000µm apart. Sections were stained by hematoxylin and eosin (H&E) and examined for frequency and cross-sectional GALT area. For immunohistochemical or immunofluorescent (IF) analyses of cell types associated with the epithelium, cells were counted in or immediately adjacent to the distal-most 100 crypts, respectively. For quantification of cell types within GALTs, cell counts were normalized to GALT cross-sectional area for the distalmost five GALTs. For evaluation of tumor development and inflammation, a collaborating expert pathologist (MKW), who was blinded to mouse genotype, examined six sections per mouse that were each 200µm apart for presence and number of invasive tumors as well as histologic scoring of colitis as previously described¹⁷.

Flow Cytometry

Five SMAD4+ *Ccr6^{GFP/+}*, six SMAD4+ *Ccr6^{GFP/GFP}*, five *Smad4^{Lrig1}Ccr6^{GFP/+}*, and four *Smad4^{Lrig1}Ccr6^{GFP/GFP}* mice were given three rounds of DSS in drinking water as described above. One month after conclusion of DSS treatment, the mice were euthanized, and single cells were isolated from colon epithelium and stroma^{5, 18}. Single cell suspensions from both the epithelium and stroma were aliquoted for staining in two parallel panels as displayed in Supplementary Figure 1A (BioLegend, San Diego, CA). Since fluorescence from GFP produced from the *Ccr6* promoter could not be detected directly, we used an anti-GFP antibody to detect cells that express the *Ccr6* promoter, even

in *Ccr6^{GFP/GFP}* mice that do not produce CCR6 protein (Supplementary Figure 1B). Data were collected on a 5-laser BD Biosciences LSRII Flow Cytometer (San Jose, CA) in the VUMC Flow Cytometry Shared Resource Core.

Statistics

In silico analysis of gene expression data in human biopsy samples were compared using the non-parametric Kruskal-Wallis test with post hoc Welch's *t* test (IBD specimens), non-parametric Mann-Whitney test (TCGA specimens), or non-parametric Spearman's correlation (IBD and TCGA specimens), as appropriate. Mann-Whitney U test was used to compare GALT area, immunostaining cell quantities, colitis inflammation scores, mean number of tumors between groups *in vivo* following DSS treatment in mice, human TMA CCR6+ cell quantification, CCL20 scoring, and human CAC mxIF immunophenotyping. Fisher's Exact test was used to compare the SMAD4 status of the human TMA samples, and the proportion of animals in each group that developed tumors following DSS treatment. Flow cytometry results were analyzed by multiple 2-tailed T test with Holm-Sidak multiple test correction. Statistical analyses were performed using GraphPad Prism 9 Software (San Diego, CA). Throughout the manuscript, statistical significance is designated as: ns (*p* .05), * (*P* < .05), and ** (*P* < .001).

Study Approval

All animal work was performed after approval by the Vanderbilt Institutional Animal Care and Use Committee. Acquired human tissue was de-identified and used with approval from the Vanderbilt Institutional Review Board.

Results

SMAD4 expression is negatively correlated with CCL20 and CCR6 expression in human IBD

Our prior work demonstrated that loss of SMAD4 in colon epithelial cells was associated with significant upregulation of multiple inflammation-related genes, including *Ccl20*⁵. Additionally, we demonstrated that *SMAD4* expression was significantly decreased in active ulcerative colitis (UCa) and active Crohn's Disease (CDa) specimens compared to healthy colon (HC) biopsy specimens analyzed by DNA Microarray (GSE75214)^{11, 12}. Analysis of the same database revealed that *CCL20* expression was significantly increased in UCa compared to UCi (inactive ulcerative colitis; *P* = .002), and that UCa, UCi, and CDa specimens demonstrated higher *CCL20* expression compared to HC (Supplementary Figure 2A). A similar analysis demonstrated that *CCR6* expression was significantly increased in UCa samples compared to UCi samples (*P* < .001), and that UCa tissue, but not UCi or CDa, contained higher expression of *CCR6* compared to HC (Supplementary Figure 2A). Furthermore, a significant inverse correlation exists between *SMAD4* and *CCL20* expression (*r* = -0.30, *P* = .001) as well as *SMAD4* and *CCR6* expression (*r* = -0.17, *P* = 0.03) in human IBD specimens (Supplementary Figure 2B).

We have previously shown that *SMAD4* expression is significantly decreased in colon cancer (CC) specimens relative to healthy colon (HCc) specimens by analysis of the TCGA

COAD colorectal cancer database¹². Analysis of the same database revealed that *CCL20* was significantly increased in CC compared to HCc specimens, and there was a significant negative correlation between *SMAD4* and *CCL20* expression in these tissues ($r^2 = -0.24$, $P < .001$; Supplementary Figure 2C). We observed a similar relationship in rectal cancer (RC) by TCGA analysis ($r^2 = -0.299$, $P = .001$; Supplementary Figure 2D). Thus, the relationship that we previously observed between *Smad4* and *Ccl20* expression in mouse colons is reflected in human IBD and sporadic CRC.

To determine the relationship of SMAD4, CCL20, and CCR6 with IBD and UCAC, we performed IHC on human TMAs. We found that UCACs exhibited significantly more CCR6+ stromal cells, greater CCL20 staining intensity, and a higher percentage of epithelium with CCL20 expression as compared to UC-dysplasia specimens, UC samples, and healthy control (Figure 1A, Supplementary Figure 3A-D). Immunohistochemical examination of SMAD4 revealed that UCACs (32.4%) were more likely to lack SMAD4 as compared to UC-dysplasia (5.6%), UC (0%), or healthy colon control (0%) (Supplementary Figure 3E; $P < .001$). Furthermore, UCAC samples with no detectable epithelial SMAD4 expression had significantly more stromal CCR6+ cells ($P = .03$; $P = .008$), higher CCL20 intensity scores ($P = .02$; $P = .04$), and higher proportion of CCL20+ epithelial cells ($P = .001$; $P < .001$) than SMAD4 cytoplasm positive and nuclear positive samples (Figure 1B-D).

To investigate whether loss of SMAD4 and associated increase in CCL20 expression and CCR6+ cells is associated with an altered immune cell infiltration in colitis-associated cancers, we performed multiplexed immunofluorescence (mxIF) on a tissue microarray containing three tissue cores from three SMAD4- and seven cores from four SMAD4+ human UCAC specimens. We found that SMAD4- UCACs exhibited an increase in overall T cell infiltration (particularly CD4+ T cells), as well as CD11b+ monocytes, CD68+ macrophages, and CD20+ B cells normalized to total tissue area when compared to SMAD4+ human UCACs (Figure 2A-B, Supplementary Figure 4). Examining specific tissue compartments, we found that the stroma surrounding, but not in contact with the epithelium, in SMAD4- UCACs exhibited a greater number of CD11b+ monocytes, CD68+ macrophages, and CD20+ B cells compared to SMAD4+ tumors coincident with significantly increased epithelium-associated CD3+ and CD4+ T cells (Figure 2C-D). These observations suggest that loss of epithelial cell SMAD4 alters key immune regulators both in close association to epithelium, as well as throughout the tumor microenvironment. In consideration of these findings in human UCACs, we further explored the effect of colon epithelial cell *Smad4* loss in the mouse colon and in the setting of colitis in mice.

Intestinal Epithelial Smad4 loss results in increased expression of inflammatory signaling genes in mouse colonic stroma, including Ccr6

To examine how increased epithelial inflammatory signaling in the setting of *Smad4* loss impacts stromal composition under homeostatic conditions, we performed bulk RNAseq on the isolated sub-epithelial stroma from three *Smad4^{Lrig1}* (lacking epithelial *Smad4* expression) and three SMAD4+ control mice. 95 genes were upregulated at least 2.5-fold ($> 1.32 \text{ Log}_2 \text{ Fold Change}$) with a false discovery rate of < 0.05 (Supplementary Figure 5A, Supplementary Table 2). Of those 95 genes, 51 are known to be expressed in immune

cells or have immune-related functions (Supplementary Table 3). Ingenuity pathway analysis demonstrated that the top 15 most significantly altered signaling pathways are immune-related, including pathways related to Th1/Th2 signaling, B cell development, leukocyte extravasation, and DC maturation, among others (Supplementary Figure 5B). ImmuCC analysis of the RNA-seq data predicted a relative increase in B cells and CD4+ T cells and a simultaneous relative decrease in CD8+ T cells and monocytes in the colonic stroma of *Smad4*^{Lrig1} mice relative to SMAD4+ controls (Supplementary Figure 5C). Among the upregulated stromal genes detected were chemokine receptors, including *Ccr7*, *Cxcr4*, *Cxcr5*, and *Ccr6*, the latter of which encodes the CCL20 receptor, CCR6 (Supplementary Tables 2-3). RNAScope *In situ* hybridization confirmed that *Smad4*^{Lrig1} mice exhibited significantly more *Ccr6*+ stromal cells relative to SMAD4+ mice (265.2 vs 94.8 cells/100 crypts, $P < .001$; Supplementary Figure 5D). These findings, together with our prior findings that loss of epithelial SMAD4 increases CCL20 expression⁵, suggest that *Smad4* loss in colon epithelial cells results in a pro-inflammatory stromal response involving the CCL20/CCR6 signaling axis.

Smad4 loss results in altered GALT phenotype, which is dependent on an intact CCL20/CCR6 axis

GALTs have a critical role in mucosal immunity, serving as major sites of T and B cell recruitment and activation, antigen sampling, and induction of local immune responses¹⁹. CCL20 is produced by follicle-associated epithelial (FAE) cells that cover the dome of GALTs where it is thought to contribute to recruitment of CCR6+ leukocytes, particularly B cells, T cells, and DCs, to GALTs^{20, 21}. RNAScope *In situ* hybridization demonstrated that *Smad4*^{Lrig1} mice exhibited significantly increased *Ccl20* expression in the follicle-associated epithelial cells immediately adjacent to GALTs compared to SMAD4+ mice (35.3 vs 12.2 mRNA copies/positive cell, $P < .001$; Supplementary Figure 6A). To determine if the increased *Ccl20* expression occurring with loss of colon epithelial *Smad4* is associated with alterations in GALT morphology, we examined the colons of five *Smad4*^{Lrig1} and five SMAD4+ control mice for frequency and size of GALTs under homeostatic conditions. While *Smad4*^{Lrig1} mice did not exhibit significantly more GALTs per colon than SMAD4+ control mice (17.2 vs 14.7, $P = .35$), GALTs in *Smad4*^{Lrig1} mice were significantly larger than GALTs in SMAD4+ control mice ($6.13 \times 10^4 \mu\text{m}^2$ vs $4.80 \times 10^4 \mu\text{m}^2$, $P = .005$; Figure 3A).

To determine if the altered GALT morphology persisted with inflammation and was dependent on CCR6 expression, the same analysis was performed in four SMAD4+ *Ccr6*^{GFP/+}, six SMAD4+ *Ccr6*^{GFP/GFP}, eight *Smad4*^{Lrig1} *Ccr6*^{GFP/+}, and eleven *Smad4*^{Lrig1} *Ccr6*^{GFP/GFP} mice 3 months after completion of DSS-induced colitis, which is when *Smad4*^{Lrig1} typically develop CACs⁵. This analysis once again demonstrated that there were no significant differences in the average number of GALTs observed across mice from all four genotypes ($P = .95$; Figure 3B). However, loss of *Ccr6* decreased GALT size irrespective of *Smad4* status, with SMAD4+ *Ccr6*^{GFP/+} mice having significantly larger GALTs than SMAD4+ *Ccr6*^{GFP/GFP} mice ($5.2 \times 10^4 \mu\text{m}^2$ vs $3.7 \times 10^4 \mu\text{m}^2$, $P = .02$) and *Smad4*^{Lrig1} *Ccr6*^{GFP/+} mice having larger GALTs than *Smad4*^{Lrig1} *Ccr6*^{GFP/GFP} mice ($7.3 \times 10^4 \mu\text{m}^2$ vs $4.4 \times 10^4 \mu\text{m}^2$, $P < .001$; Figure 3B, Supplementary Figure 6B). These findings

are consistent with previous reports that CCR6 serves a critical role in GALT development and immune cell trafficking in the mouse colon ^{6, 22}. On the other hand, loss of *Smad4* increased GALT size when *Ccr6* was expressed, with *Smad4^{Lrig1} Ccr6^{GFP/+}* mice having larger GALTs than SMAD4+ *Ccr6^{GFP/+}* mice ($7.3 \times 10^4 \mu\text{m}^2$ vs $5.2 \times 10^4 \mu\text{m}^2$, $P = .007$; Figure 3B) and this gain was blocked by loss of *Ccr6*. DSS treatment alone appeared to have little effect on GALT size when comparing SMAD4+ *Ccr6^{+/+}* mice without DSS treatment and SMAD4+ *Ccr6^{GFP/+}* mice treated with DSS ($4.80 \times 10^4 \mu\text{m}^2$ vs. $5.2 \times 10^4 \mu\text{m}^2$; $P = .07$), assuming there is no effect of loss of one copy of *Ccr6*. However, differences were seen in DSS response when SMAD4 was lost from epithelium. *Smad4^{Lrig1} Ccr6^{GFP/+}* mice demonstrated larger GALTs after induction of colitis compared to *Smad4^{Lrig1} Ccr6^{+/+}* mice under homeostatic conditions ($7.3 \times 10^4 \mu\text{m}^2$ vs $6.13 \times 10^4 \mu\text{m}^2$; $P = .04$). While comparison of mice with or without DSS treatment is complicated by the loss of one allele of *Ccr6* under DSS conditions and by the cohorts generated at different times, they are consistent with our data that SMAD4 modulates immune responses.

IF staining for GFP as a marker of *Ccr6* promoter activity revealed that an expansion of the CCR6+ cell population contributed to the larger GALT size in the context of SMAD4 loss. GALTs in *Smad4^{Lrig1} Ccr6^{GFP/+}* mice consisted of a significantly higher proportion of GFP+ cells compared to SMAD4+ *Ccr6^{GFP/+}* mice (72.9% vs 50.9%, $P < .001$; Figure 3C) and this increase was offset by additional loss of *Ccr6* in *Smad4^{Lrig1} Ccr6^{GFP/GFP}* mice (72.9% vs 35.8%, $P < .001$). Thus, loss of epithelial SMAD4 expression leads to larger GALTs with increased proportions of CCR6+ immune cells that is dependent on *Ccr6* expression. To understand whether SMAD4 signaling alters the distribution or quantity of different immune cell types within the GALTs, IF staining was performed on tissue sections from five *Smad4^{Lrig1} Ccr6^{GFP/+}* and five SMAD4+ *Ccr6^{GFP/+}* mice under homeostatic conditions to localize B cells, T cells, and DCs. SMAD4 loss resulted in an increase in the number of B220+ cells (40.5% vs 29.5%, $P = .002$; Supplementary Figure 7A). The absolute numbers of CD3+ T cells and CD11c+ DCs were significantly increased in GALTs of *Smad4^{Lrig1} Ccr6^{GFP/+}* mice compared to SMAD4+ *Ccr6^{GFP/+}* mice (Supplementary Figure 7B-C). However, the proportion of these cell types within GALTs was unchanged (data not shown). B cell, T cell, and DC distributions were not altered within the GALTs. B cells remained localized to the germinal center of GALTs, while T cells were spread throughout the GALT periphery, and DCs were localized to the subepithelial dome of GALTs, regardless of CCR6 expression status (Supplementary Figure 7A-C).

Smad4 loss increases immune cell infiltration in mouse colonic stroma, particularly T cell subsets and CD11c+ DCs, that is abrogated by additional loss of Ccr6

To understand how epithelial *Smad4* loss impacts recruitment of specific immune cell types and to what degree these changes depend on functional CCL20/CCR6 signaling, we analyzed mice with and without epithelial SMAD4 and with or without CCR6 one month after DSS treatment to avoid indirect effects of tumorigenesis that occurs 2–3 months post-DSS. We used flow cytometry to quantify relative changes in leukocyte populations, distinguishing epithelial-associated immune cells from those in the sub-epithelial stroma. Colitis was induced by administration of three rounds of DSS in five SMAD4+ *Ccr6^{GFP/+}*, six SMAD4+ *Ccr6^{GFP/GFP}*, five *Smad4^{Lrig1} Ccr6^{GFP/+}*, and four *Smad4^{Lrig1} Ccr6^{GFP/GFP}*

mice. Parallel myeloid and lymphoid flow cytometry staining panels were used to characterize the compositions of each compartment one month after the end of DSS treatment to determine changes in immune cell recruitment that may contribute to CAC formation.

Within the colonic stroma, loss of *Ccr6* alone had little effect on the immune populations examined. However, a number of changes in immune cell composition were observed with epithelial cell loss of *Smad4*. *Smad4^{Lrig1} Ccr6^{GFP/+}* mice demonstrated a greater than two-fold increase in proportion of CD45⁺ immune cells in the colonic stromal tissues when compared to *SMAD4⁺ Ccr6^{GFP/+}* mice (41.4% vs 19.6%, $P < .001$) and this increase was abrogated by loss of *Ccr6* (*Smad4^{Lrig1} Ccr6^{GFP/+}* mice 41.4% vs. *Smad4^{Lrig1} Ccr6^{GFP/GFP}* mice 15.6%, $P < .001$; Figure 4A-B). After normalizing to the CD45⁺ population, loss of *Smad4* alone resulted in increased CD3⁺ T cells. Among CD3⁺ T cells, the proportion of CD4⁺ T cells, CD4⁺ FoxP3⁺ Tregs, and CD4⁺ IL-17a⁺ cells were increased in the context of *Smad4* loss, but these increases were dependent upon *Ccr6* expression (Figure 4C-E). *Smad4^{Lrig1} Ccr6^{GFP/+}* mice also had a significantly increased stromal CD11c⁺ population (Figure 4A, F). Further gating demonstrated that 60% of these cells were CD11b⁻ and 52% were CX3CR1⁺, both of which were significantly increased in *Smad4^{Lrig1} Ccr6^{GFP/+}* mice as compared to *SMAD4⁺* mice and these increases were also dependent upon *Ccr6* expression (Figure 4G). The expansion of these cell types in the absence of *Smad4* expression was likely due to recruitment of CCR6⁺ cells. Increases in CCR6⁺ cells marked by GFP⁺ staining within the CD45⁺, CD3⁺, CD4⁺, FoxP3⁺, IL-17a⁺, and CD11c⁺ populations mirrored the observed increases in these cell subtypes in *Smad4^{Lrig1} Ccr6^{GFP/+}* mice (Supplementary Figure 8A). Additionally, the overwhelming majority of CCR6⁺ cells identified by GFP⁺ staining via flow cytometry in *Smad4^{Lrig1} Ccr6^{GFP/+}* mice were immune cells (Supplementary Figure 8B).

To summarize the above findings, loss of epithelial SMAD4 expression leads to increased leukocyte recruitment to the colonic stroma, including CD4⁺ T cells, Tregs, T_H17 cells, CD11c⁺ CD11b⁻ DCs, and CD11c⁺ CX3CR1⁺ DCs (Supplementary Table 4). Notably, these changes are dependent on CCR6 expression, indicating that an intact CCL20/CCR6 axis is necessary to induce the stromal pro-inflammatory response observed due to epithelial SMAD4 loss.

***Ccr6* mediates *Smad4*-dependent recruitment of mouse colon epithelial-associated T_H17 and CD11c⁺ DCs**

Flow cytometric analysis was also performed on epithelial-associated cells. As in the sub-epithelial stroma, there was little effect on most of the examined populations in response to *Ccr6* loss alone. *Smad4^{Lrig1} Ccr6^{GFP/+}* mice demonstrated a significant increase in CD45⁺ cells within the colon epithelium fraction relative to *SMAD4⁺ Ccr6^{GFP/+}* mice (20.1% vs 9.6%, $P < .001$) and this increase was dependent upon *Ccr6* expression (*Smad4^{Lrig1} Ccr6^{GFP/+}* mice 20.1% vs. *Smad4^{Lrig1} Ccr6^{GFP/GFP}* mice 10.5%; $P < .001$; Figure 5A-B). While there were no observed differences in total epithelial-associated CD3⁺ cells, CD4⁺ cells, or CD4⁺ FoxP3⁺ Tregs among the four genotypes, the epithelium of *Smad4^{Lrig1} Ccr6^{GFP/+}* mice exhibited significantly more CD4⁺ IL-17a⁺ cells than

SMAD4+ *Ccr6*^{GFP/+} mice (6.4% vs 1.4%; $P < .001$) and loss of *Ccr6* abrogated this effect (*Smad4* *Lrig1* *Ccr6*^{GFP/+} mice 6.4% vs. *Smad4* *Lrig1* *Ccr6*^{GFP/GFP} mice 1.2%; $P < .001$; Figure 5A,C-E). Thus, loss of epithelial SMAD4 expression in the colon results in a shift in CD3+ T cell composition towards increased T_H17 cells. Interestingly, *Ccr6* null mice demonstrated an expansion of colon epithelial-associated CD8+ T cells regardless of SMAD4 status, thus indicating a critical role for CCR6 in limiting CD8+ T cell trafficking to the intestinal epithelium (Figure 5D).

Among the myeloid cell populations, epithelial-associated CD11c+ DCs were increased in *Smad4* *Lrig1* *Ccr6*^{GFP/+} mice relative to SMAD4+ *Ccr6*^{GFP/+} (21.9% vs 13.6%, $P = .03$), including a significant increase in the CD11c+ CX3CR1+ DC subset and these increases were also abrogated by loss of *Ccr6* (Figure 5A, F-G). The DC population observed within the epithelium differed from the stroma in that the majority of DCs associated with the epithelium were CD11c+ CD11b+, whereas the sub-epithelial stroma contained primarily CD11c+ CD11b- DCs. Further gating for GFP expression among these cell types demonstrated a concomitant increase in GFP+ cells among the increased T_H17 and dendritic cell populations (Supplementary Figure 9A). Similar to stroma, the increase in CCR6+ cells seen with colon epithelial cell SMAD4 loss were overwhelmingly CD45+ (Supplementary Figure 9B).

In summary, loss of colon epithelial cell SMAD4 leads to increased recruitment of specific immune cell subsets within the epithelium, particularly T_H17 cells and DCs including CD11c+ CD11b+ and CD11c+ CX3CR1+ DC subtypes that is dependent on CCR6 activity (Supplementary Table 4). *Ccr6* loss led to an increase in CD8+ IELs regardless of SMAD4 expression status as previously published^{13, 23}.

CAC susceptibility due to SMAD4 loss is dependent on the CCL20/CCR6 axis

We previously published that loss of epithelial SMAD4 in the colon significantly predisposes mice to CAC within three months of DSS-induced chronic inflammation, and that these tumors are morphologically similar to human UCACs⁵. To determine if this cancer susceptibility phenotype also depends on an intact CCL20/CCR6 axis, we induced chronic colitis in two SMAD4+ *Ccr6*^{GFP/+}, six SMAD4+ *Ccr6*^{GFP/GFP}, eight *Smad4* *Lrig1* *Ccr6*^{GFP/+}, and 11 *Smad4* *Lrig1* *Ccr6*^{GFP/GFP} mice with 3 cycles of DSS. Three months after completion of DSS treatment, 100% (8 of 8) of *Smad4* *Lrig1* *Ccr6*^{GFP/+} mice developed adenocarcinomas of the colon with invasion deep into the submucosa, consistent with prior observations from our group (Figure 6A)⁵. In contrast, only 18.2% (2 of 11) *Smad4* *Lrig1* *Ccr6*^{GFP/GFP} mice developed these invasive cancers, one of which was characterized as a single invasive crypt. There were no differences in tumor formation between sexes as previously shown (Supplementary Table 5)⁵. Thus, loss of CCR6 expression is associated with a significant decrease in susceptibility to CAC development in *Smad4* null mice (100.0 vs 18.2%, $P < .001$) Loss of *Ccr6* expression was similarly associated with fewer invasive tumors per colon (Figure 6B). The range of invasive adenocarcinomas for *Smad4* *Lrig1* *Ccr6*^{GFP/+} mice was 1 – 3 tumors compared to 0 – 2 invasive adenocarcinomas per colon in *Smad4* *Lrig1* *Ccr6*^{GFP/GFP} mice. We did note a single invasive crypt on a single section of one SMAD4+ *Ccr6*^{GFP/GFP} mouse, consistent with previous observations that DSS-induced

colitis can occasionally induce tumorigenesis in mice without loss of SMAD4 but at longer time points (Figure 6C) ²⁴.

Tissue sections from the same mice were subjected to histologic grading of colitis. Among the *Smad4*^{Lrig1} mice, there was no significant difference between *Ccr6* expressing and *Ccr6* null mice in terms of weight loss during DSS or overall inflammation score at the time of tumor scoring (data not shown). However, in SMAD4+ control mice, *Ccr6* expression was associated with a higher percentage of crypts involved with colitis (2 vs 1.17, $P = .03$) and deeper crypt damage (2 vs 1.67, $P = .004$) compared to *Ccr6* null mice. Loss of *Smad4* also decreased the severity of colitis; SMAD4+ *Ccr6*^{GFP/+} mice had higher average crypt damage scores than *Smad4*^{Lrig1} *Ccr6*^{GFP/+} mice (2 vs 0.5, $P < .001$) and a similar relationship was observed between SMAD4+ *Ccr6*^{GFP/GFP} and *Smad4*^{Lrig1} *Ccr6*^{GFP/GFP} mice (1.67 vs 0.46, $P = .002$; Supplementary Table 6).

Thus, loss of *Smad4* reduced histologic evidence of the severity of ongoing colitis yet contributed to the development of invasive tumors at a higher rate and frequency. These findings indicate that the development of CAC in *Smad4*^{Lrig1} *Ccr6*^{GFP/+} mice is not solely dependent on the severity of colitis alone, but rather on the unique response to colitis seen with epithelial SMAD4 loss.

Altered immune cell landscape in the setting of SMAD4 loss persists with tumorigenesis

The above data suggest that loss of epithelial SMAD4 promotes a unique immune microenvironment within one month of induction of chronic colitis and leads to a profound susceptibility to CAC development by three months, both of which are dependent on CCR6 expression. To determine if the observed immune cell changes are transient or persist through tumorigenesis, we performed IHC of specific immune cell subtypes in SMAD4+ *Ccr6*^{GFP/+}, SMAD4+ *Ccr6*^{GFP/GFP}, *Smad4*^{Lrig1} *Ccr6*^{GFP/+}, and *Smad4*^{Lrig1} *Ccr6*^{GFP/GFP} mice 3 months after completion of DSS treatment. Overall, the unique immunophenotype observed in *Smad4*^{Lrig1} *Ccr6*^{GFP/+} mice one month after DSS completion persisted at three months after DSS completion in regions adjacent to tumors. CD3+ cells were increased throughout the GALTs with loss of *Smad4* only when *Ccr6* was expressed. Within the epithelium, a similar number of CD3+ T cells were observed with or without loss of *Smad4* or *Ccr6* (Supplementary Figure 10A). Examination of CD8+ IELs by IHC at three months corroborated our flow cytometry results that *Ccr6* loss leads to increased CD8+ IELs regardless of SMAD4 status (Supplementary Figure 10B).

FoxP3+ Tregs were noted to be localized to GALTs or adjacent to epithelium, without significant distribution through the rest of the stroma (Figure 7A). Within the GALTs, FoxP3+ Tregs were markedly increased in *Smad4*^{Lrig1} *Ccr6*^{GFP/+} mice but not in *Smad4*^{Lrig1} *Ccr6*^{GFP/GFP} mice (Figure 7A). Similar to mice at one month after DSS treatment, there was no observable difference in epithelial-associated Tregs (Figure 7B). IL17+ cells were notably increased in the GALTs and epithelium following *Smad4*^{Lrig1} loss but only in the presence of *Ccr6* expression. (Supplementary Figure 11A-B). The distribution of CD11c+ DCs was similar among mice from all four genotypes (Supplementary Figure 12). Together, our findings indicate that epithelial SMAD4 loss induces immunophenotypic changes that persist from after DSS treatment when no tumors

are detectable through 3 months after DSS when invasive cancers are prevalent in all of the *Smad4^{Lrig1 Ccr6^{GFP/+}}* mice. Both the immune cell changes and tumorigenesis are blocked by loss of *Ccr6*, linking the immune phenotype to tumorigenesis.

Discussion

Multiple defects in the TGF β signaling pathway, including receptor mutations and mutations in *SMAD* genes, most frequently *SMAD4*, have been previously implicated in multiple gastrointestinal pathologies including human IBD and CRC^{4, 25, 26}. Previous attention has primarily focused on the roles of TGF β in maintenance of epithelial homeostasis including regulation of cell growth, cell cycle, differentiation, and apoptosis, all of which likely factor into the tumor suppressor effects of TGF β family signaling^{27, 28}. Our data support a novel tumor suppressor function of the canonical TGF β signaling pathway via modulation of inflammatory responses in the epithelium. It is already well appreciated that the TGF β signaling pathway plays an important immunosuppressive role through its direct actions on immune cells, including inhibition of T_h1 helper cell, cytotoxic T cell, and NK cell responses, and simultaneous promotion of Treg differentiation and function.^{29, 30} Here, we add another level of homeostatic immune regulation by TGF β signaling via direct effects on epithelium, downregulating epithelial inflammatory genes, particularly *Ccl20*, to suppress specific mucosal inflammatory responses and inflammation-associated carcinogenesis.

Several studies have implicated defective epithelial TGF β signaling or the CCL20/CCR6 axis in IBD and CRC development^{31, 32}. However, we have identified for the first time a significant inverse correlation between levels of *SMAD4* and both *CCL20* and *CCR6* mRNAs in human IBD. As expected for its tumor suppressor role, loss of epithelial *SMAD4* is more common in UCACs than UC-dysplasia, UC, or healthy colon controls and loss of epithelial *SMAD4* in these tumors results in increased epithelial CCL20 protein expression and stromal CCR6+ cells compared to *SMAD4*+ tumors. Consistent with UCAC results, *CCL20* expression is also inversely correlated with *SMAD4* expression in sporadic colon and rectal cancer. By utilizing our conditional, tissue-specific *Smad4* knockout model, we have been able to link the epithelial function of *SMAD4* to regulation of CCL20/CCR6 signaling, suggesting a mechanism underlying inflammation and tumorigenesis downstream of decreased or lost TGF β /*SMAD4* signaling in human patients along the IBD to CAC spectrum. Given these findings, it is intriguing to speculate about a role for CCL20/CCR6 pathway in patients with germline mutations or deletions of *SMAD4*, such as in juvenile polyposis syndrome, but further research is needed³³.

Concurrent with increased chemokine/cytokine expression in *Smad4* null mouse colon epithelium is an increase in pro-inflammatory signaling within the underlying stroma. Many of the upregulated genes in the stroma have known roles in the innate and adaptive immune responses, including those involved with mucosal immune trafficking and GALT structure and function. Additionally, we observed evidence of increased GALT size in *Smad4^{Lrig1}* mice. CCL20 signaling to CCR6 is known to regulate immune cell trafficking to mucosa-associated lymphoid structures such as GALTs³⁴. Consistent with this concept, not only did GALT size increase with increased CCL20 expression after loss of epithelial *SMAD4* loss, but this increase in GALT size was abrogated in mice without *Ccr6* expression. Increased

Ccl20 expression, *Ccr6* expression, and GALT size, and upregulation of genes that function in pathogen recognition (*Tlr9*, *Pyhin2*, *Fcrla*, *Ly86*) support a role for the SMAD4-mediated regulation of CCL20 in modulating mucosal immune responses through GALT activity.

Herein we demonstrated that much of the inflammatory response to *Smad4* loss in the epithelium can be abrogated by loss of *Ccr6*, which is normally expressed on many of the immune cells that are increased with epithelial SMAD4 loss. The reduction in tumor burden in response to *Ccr6* deletion in *Smad4^{Lrig1}* mice suggests the CCL20/CCR6 axis is one of the most critical inflammatory pathways downstream of TGF β signaling in the development of CAC. Our findings are consistent with previous findings that loss of *Ccr6* expression protects against *APC* mutant-driven and azoxymethane (AOM)/DSS-driven tumorigenesis in mice³⁵. While restoring expression of tumor suppressor genes remains clinically intractable, targeting downstream pathways such as CCL20/CCR6 may be one approach for more selective clinically-targeted therapies.

Our findings additionally provide insight into immune cell subtypes downstream of SMAD4 loss that could be targeted for improved therapies for prevention of or treatment of CACs. Our results suggest that targeted therapy against CCR6 may be effective in preventing CAC in ulcerative colitis patients. There may also be efficacy in targeting specific cell types that respond to CCR6 activation. In particular, we observed an increase in stromal Tregs, T_H17 cells, and DCs as well as epithelial-associated T_H17 cells and DCs in *Smad4^{Lrig1}* mice (summarized in Supplementary Table 4). Tregs are involved in suppressing immune responses, particularly against commensal bacteria in the gut. However, the immunomodulatory role of Tregs may hinder tumor immunosurveillance and thereby contribute to tumor formation³⁶. Several studies have shown that Tregs are more abundant in inflamed IBD colon mucosa and in colon tumors compared to non-inflamed or healthy colon samples in humans^{37, 38}. We observed increased Tregs in the stroma of *Smad4^{Lrig1}* mice after induction of inflammation at the time of CAC formation and before tumors developed, suggesting a potential role of Tregs in CAC tumorigenesis.

In the present study, we also observed an increased number of T_H17 cells in both the stromal and epithelial compartments of *Smad4^{Lrig1}* mice. While the role of T_H17 cells in tumor immunity remains poorly understood, immunoneutralization of IL-17 has been shown to inhibit colitis and CAC formation in an enterotoxigenic colitis mouse model³⁹. Thus, two CCR6+ immune cells, T_H17 cells and FoxP3+ Tregs, are candidate effector cell types which may play a causative role in colitis-associated tumorigenesis due to SMAD4 loss and CCL20 secretion. Additionally, we also observed increased CD11c+ CX3CR1+ cells in the epithelial and stromal compartment of *Smad4^{Lrig1}* mice with intact CCR6 expression. CD11c+ CX3CR1+ cells have previously been observed in the mucosa of IBD patients and are known to produce both IL-1 and IFN β , which are required for T_H17 cell differentiation and Treg expansion, respectively^{40, 41}. Future studies will define which of these CCR6+ cell types are critical to tumorigenesis and whether they could be targeted clinically in the setting of colitis.

The stroma and epithelium of *Smad4^{Lrig1} Ccr6^{GFP/+}* mice demonstrated several differences in immune cell infiltration that highlight known interactions between immune cell types

that may promote tumorigenesis. Within GALTs, DCs activate and stimulate T cell differentiation and migration^{42, 43}, which can result in induction of specific T cell populations and subsequent migration toward colonic epithelium. Thus, loss of epithelial SMAD4 and subsequent increase in CCL20/CCR6 signaling affects not only GALT-specific cells, but also the lymphocytes that then migrate out of the GALTs into surrounding stroma and/or to the epithelium. Our data suggest that the CCL20/CCR6 axis mediates activation and migration of Treg, Th17, and CD8+ T cells with Treg cells migrating into surrounding stroma, and Th17 and CD8+ T cells migrating both to epithelium and throughout the stroma. Several studies have implicated IL-17a in tumor growth and progression due its contributions to wound healing, regeneration, and barrier function⁴⁴⁻⁴⁶. Thus, direct interaction of Th17 cells with epithelium seen within SMAD4 deficiency in both humans and mice may contribute to cancer progression. Future experiments will determine how these specific immune cell types promote tumorigenesis in the setting of colitis and SMAD4 loss.

In summary, we have identified a specific chemokine pathway, epithelial CCL20 signaling to CCR6 on immune cells, that is normally inhibited by TGF β family canonical signaling under homeostatic conditions but is activated by epithelial loss of SMAD4 in the colon and is essential for the development of CAC in conditional *Smad4* knockout mice. We have also identified the specific inflammatory cells that respond to that chemokine axis and correlate with carcinogenesis. Future research will identify how specific immune cell functional alterations in the context of epithelial loss of SMAD4 expression contribute to colon epithelial cell transformation and cancer progression and whether these represent potential opportunities in the prevention or treatment of colorectal cancer.

Supplementary Material

Refer to Web version on PubMed Central for supplementary material.

Acknowledgments

Grant Support: This work was supported in part by National Cancer Institute grants (F32CA236309; T32CA106183; R01CA235016, R01CA200681, P30CA68485, and P30DK058404) and the Burroughs Wellcome Fund Physician-Scientist Institutional Award (#1018894)/Vanderbilt Supporting Careers in Research for Interventional Physicians and Surgeons. The authors would also like to acknowledge the institutional shared resources and core facilities that made this research possible (Vanderbilt University, Nashville, Tennessee, USA), including the Vanderbilt Technologies for Advanced Genomics (VANTAGE), the Digital Histology Shared Resource (DHSR), the Cell Imaging Shared Resource (CISR), and the Flow Cytometry Shared Resource (FCSR).

Abbreviations:

| | |
|------------------------------|------------------------------------|
| CRC | colorectal cancer |
| IBD | inflammatory bowel disease |
| TGFβ | transforming growth factor β |
| CAC | colitis-associated carcinoma |
| CCL20 | c-c motif chemokine ligand 20 |

| | |
|-------------|--------------------------------------|
| CCR6 | c-c motif chemokine receptor 6 |
| GALT | gut-associated lymphoid tissue |
| DSS | dextran sodium sulfate |
| TMA | tissue microarray |
| UCAC | ulcerative colitis-associated cancer |
| IHC | immunohistochemistry |
| IF | immunofluorescent |
| UCa | active ulcerative colitis |
| CDa | active Crohn's disease |
| HC | healthy colon |
| UCi | inactive ulcerative colitis |
| TCGA | the cancer genome atlas |
| CC | colon cancer |
| HCC | healthy colon control |
| RC | rectal cancer |
| MxIF | multiplex immunofluorescence |
| FAE | follicle-associated epithelium |

References

1. Elinav E, Nowarski R, Thaiss CA, et al. Inflammation-induced cancer: crosstalk between tumours, immune cells and microorganisms. *Nat Rev Cancer* 2013;13:759–71. [PubMed: 24154716]
2. Siegel RL, Miller KD, Goding Sauer A, et al. Colorectal cancer statistics, 2020. *CA Cancer J Clin* 2020;70:145–164. [PubMed: 32133645]
3. Coussens LM, Werb Z. Inflammation and cancer. *Nature* 2002;420:860–7. [PubMed: 12490959]
4. Smith PM, Means AL, Beauchamp RD. Immunomodulatory Effects of TGF-beta Family Signaling within Intestinal Epithelial Cells and Carcinomas. *Gastrointest Disord (Basel)* 2019;1:290–300. [PubMed: 33834163]
5. Means AL, Freeman TJ, Zhu J, et al. Epithelial Smad4 Deletion Up-Regulates Inflammation and Promotes Inflammation-Associated Cancer. *Cell Mol Gastroenterol Hepatol* 2018;6:257–276. [PubMed: 30109253]
6. Comerford I, Bunting M, Fenix K, et al. An immune paradox: how can the same chemokine axis regulate both immune tolerance and activation?: CCR6/CCL20: a chemokine axis balancing immunological tolerance and inflammation in autoimmune disease. *Bioessays* 2010;32:1067–76. [PubMed: 20954179]
7. Wang L, Liu Q, Sun Q, et al. TLR4 signaling in cancer cells promotes chemoattraction of immature dendritic cells via autocrine CCL20. *Biochem Biophys Res Commun* 2008;366:852–6. [PubMed: 18083111]

8. Frick VO, Rubie C, Kolsch K, et al. CCR6/CCL20 chemokine expression profile in distinct colorectal malignancies. *Scand J Immunol* 2013;78:298–305. [PubMed: 23790181]
9. Skovdahl HK, Granlund A, Ostvik AE, et al. Expression of CCL20 and Its Corresponding Receptor CCR6 Is Enhanced in Active Inflammatory Bowel Disease, and TLR3 Mediates CCL20 Expression in Colonic Epithelial Cells. *PLoS One* 2015;10:e0141710. [PubMed: 26536229]
10. Zhang H, Zhong W, Zhou G, et al. Expression of chemokine CCL20 in ulcerative colitis. *Mol Med Rep* 2012;6:1255–60. [PubMed: 23008075]
11. Vancamelbeke M, Vanuytsel T, Farre R, et al. Genetic and Transcriptomic Bases of Intestinal Epithelial Barrier Dysfunction in Inflammatory Bowel Disease. *Inflamm Bowel Dis* 2017;23:1718–1729. [PubMed: 28885228]
12. Marincola Smith P, Choksi YA, Markham NO, et al. Colon epithelial cell TGFbeta signaling modulates the expression of tight junction proteins and barrier function in mice. *Am J Physiol Gastrointest Liver Physiol* 2021;320:G936–G957. [PubMed: 33759564]
13. Lugerling A, Ross M, Sieker M, et al. CCR6 identifies lymphoid tissue inducer cells within cryptopatches. *Clin Exp Immunol* 2010;160:440–9. [PubMed: 20148914]
14. Edgar R, Domrachev M, Lash AE. Gene Expression Omnibus: NCBI gene expression and hybridization array data repository. *Nucleic Acids Res* 2002;30:207–10. [PubMed: 11752295]
15. Barrett T, Wilhite SE, Ledoux P, et al. NCBI GEO: archive for functional genomics data sets--update. *Nucleic Acids Res* 2013;41:D991–5. [PubMed: 23193258]
16. Means AL, Ray KC, Singh AB, et al. Overexpression of heparin-binding EGF-like growth factor in mouse pancreas results in fibrosis and epithelial metaplasia. *Gastroenterology* 2003;124:1020–36. [PubMed: 12671899]
17. Dieleman LA, Palmén MJ, Akol H, et al. Chronic experimental colitis induced by dextran sulphate sodium (DSS) is characterized by Th1 and Th2 cytokines. *Clin Exp Immunol* 1998;114:385–91. [PubMed: 9844047]
18. Banerjee A, Herring CA, Chen B, et al. Succinate Produced by Intestinal Microbes Promotes Specification of Tuft Cells to Suppress Ileal Inflammation. *Gastroenterology* 2020;159:2101–2115 e5. [PubMed: 32828819]
19. Habtezion A, Nguyen LP, Hadeiba H, et al. Leukocyte Trafficking to the Small Intestine and Colon. *Gastroenterology* 2016;150:340–54. [PubMed: 26551552]
20. Rhee KJ, Jasper PJ, Sethupathi P, et al. Positive selection of the peripheral B cell repertoire in gut-associated lymphoid tissues. *J Exp Med* 2005;201:55–62. [PubMed: 15623575]
21. Morbe UM, Jorgensen PB, Fenton TM, et al. Human gut-associated lymphoid tissues (GALT); diversity, structure, and function. *Mucosal Immunol* 2021;14:793–802. [PubMed: 33753873]
22. Kucharzik T, Hudson JT 3rd, Waikel RL, et al. CCR6 expression distinguishes mouse myeloid and lymphoid dendritic cell subsets: demonstration using a CCR6 EGFP knock-in mouse. *Eur J Immunol* 2002;32:104–12. [PubMed: 11754009]
23. Varona R, Villares R, Carramolino L, et al. CCR6-deficient mice have impaired leukocyte homeostasis and altered contact hypersensitivity and delayed-type hypersensitivity responses. *J Clin Invest* 2001;107:R37–45. [PubMed: 11254677]
24. Okayasu I, Yamada M, Mikami T, et al. Dysplasia and carcinoma development in a repeated dextran sulfate sodium-induced colitis model. *J Gastroenterol Hepatol* 2002;17:1078–83. [PubMed: 12201867]
25. Gough NR, Xiang X, Mishra L. TGF-beta Signaling in Liver, Pancreas, and Gastrointestinal Diseases and Cancer. *Gastroenterology* 2021;161:434–452 e15. [PubMed: 33940008]
26. Ikushima H, Miyazono K. TGFbeta signalling: a complex web in cancer progression. *Nat Rev Cancer* 2010;10:415–24. [PubMed: 20495575]
27. Principe DR, Doll JA, Bauer J, et al. TGF-beta: duality of function between tumor prevention and carcinogenesis. *J Natl Cancer Inst* 2014;106:djt369. [PubMed: 24511106]
28. Roberts AB, Wakefield LM. The two faces of transforming growth factor beta in carcinogenesis. *Proc Natl Acad Sci U S A* 2003;100:8621–3. [PubMed: 12861075]
29. Yang L, Pang Y, Moses HL. TGF-beta and immune cells: an important regulatory axis in the tumor microenvironment and progression. *Trends Immunol* 2010;31:220–7. [PubMed: 20538542]

30. Travis MA, Sheppard D. TGF-beta activation and function in immunity. *Annu Rev Immunol* 2014;32:51–82. [PubMed: 24313777]
31. Massague J. TGF-beta signaling in development and disease. *FEBS Lett* 2012;586:1833. [PubMed: 22651913]
32. Monteleone G, Kumberova A, Croft NM, et al. Blocking Smad7 restores TGF-beta1 signaling in chronic inflammatory bowel disease. *J Clin Invest* 2001;108:601–9. [PubMed: 11518734]
33. Brosens LA, Langeveld D, van Hattem WA, et al. Juvenile polyposis syndrome. *World J Gastroenterol* 2011;17:4839–44. [PubMed: 22171123]
34. Williams IR. CCR6 and CCL20: partners in intestinal immunity and lymphorganogenesis. *Ann N Y Acad Sci* 2006;1072:52–61. [PubMed: 17057190]
35. Wunderlich CM, Ackermann PJ, Ostermann AL, et al. Obesity exacerbates colitis-associated cancer via IL-6-regulated macrophage polarisation and CCL-20/CCR-6-mediated lymphocyte recruitment. *Nat Commun* 2018;9:1646. [PubMed: 29695802]
36. Li L, Boussiotis VA. The role of IL-17-producing Foxp3+ CD4+ T cells in inflammatory bowel disease and colon cancer. *Clin Immunol* 2013;148:246–53. [PubMed: 23773923]
37. Ghazalsafala R, Rezaee SA, Rafatpanah H, et al. Evaluation of CD4+ CD25+ FoxP3+ Regulatory T cells and FoxP3 and CTLA-4 gene Expression in Patients with Newly Diagnosed Tuberculosis in Northeast of Iran. *Jundishapur J Microbiol* 2015;8:e17726. [PubMed: 26034548]
38. Maul J, Loddenkemper C, Mundt P, et al. Peripheral and intestinal regulatory CD4+ CD25(high) T cells in inflammatory bowel disease. *Gastroenterology* 2005;128:1868–78. [PubMed: 15940622]
39. Wu S, Rhee KJ, Albesiano E, et al. A human colonic commensal promotes colon tumorigenesis via activation of T helper type 17 T cell responses. *Nat Med* 2009;15:1016–22. [PubMed: 19701202]
40. Bernardo D, Marin AC, Fernandez-Tome S, et al. Human intestinal pro-inflammatory CD11c(high)CCR2(+)CX3CR1(+) macrophages, but not their tolerogenic CD11c(-)CCR2(-)CX3CR1(-) counterparts, are expanded in inflammatory bowel disease. *Mucosal Immunol* 2018;11:1114–1126. [PubMed: 29743615]
41. Gu T, Li Q, Egilmez NK. IFNbeta-producing CX3CR1(+) macrophages promote T-regulatory cell expansion and tumor growth in the APC(min+)/Bacteroides fragilis colon cancer model. *Oncoimmunology* 2019;8:e1665975. [PubMed: 31741765]
42. Tran Janco JM, Lamichhane P, Karyampudi L, et al. Tumor-infiltrating dendritic cells in cancer pathogenesis. *J Immunol* 2015;194:2985–91. [PubMed: 25795789]
43. Wang Y, Xiang Y, Xin VW, et al. Dendritic cell biology and its role in tumor immunotherapy. *J Hematol Oncol* 2020;13:107. [PubMed: 32746880]
44. Maxwell JR, Zhang Y, Brown WA, et al. Differential Roles for Interleukin-23 and Interleukin-17 in Intestinal Immunoregulation. *Immunity* 2015;43:739–50. [PubMed: 26431947]
45. Zepp JA, Zhao J, Liu C, et al. IL-17A-Induced PLET1 Expression Contributes to Tissue Repair and Colon Tumorigenesis. *J Immunol* 2017;199:3849–3857. [PubMed: 29070673]
46. Grivennikov SI, Wang K, Mucida D, et al. Adenoma-linked barrier defects and microbial products drive IL-23/IL-17-mediated tumour growth. *Nature* 2012;491:254–8. [PubMed: 23034650]

What You Need to Know

Background and Context:

SMAD4 serves an important tumor suppressor function in the colon by regulating the immune response to inflammation, and loss of colon epithelial SMAD4 is associated with colitis-associated tumor formation.

New Findings:

SMAD4 loss in mice is associated with recruitment of specific immune cells to the colon and leads to tumors only in the presence of intact CCL20/CCR6 signaling.

Limitations:

Future studies will define how CCR6+ immune cells recruited by increased CCL20 signaling in the context of SMAD4 loss cell promote tumorigenesis in the setting of colitis.

Impact:

While targeting loss of function such as SMAD4 loss remains clinically intractable, identification of downstream pathways upregulated by that loss may provide targets for better therapeutic interventions.

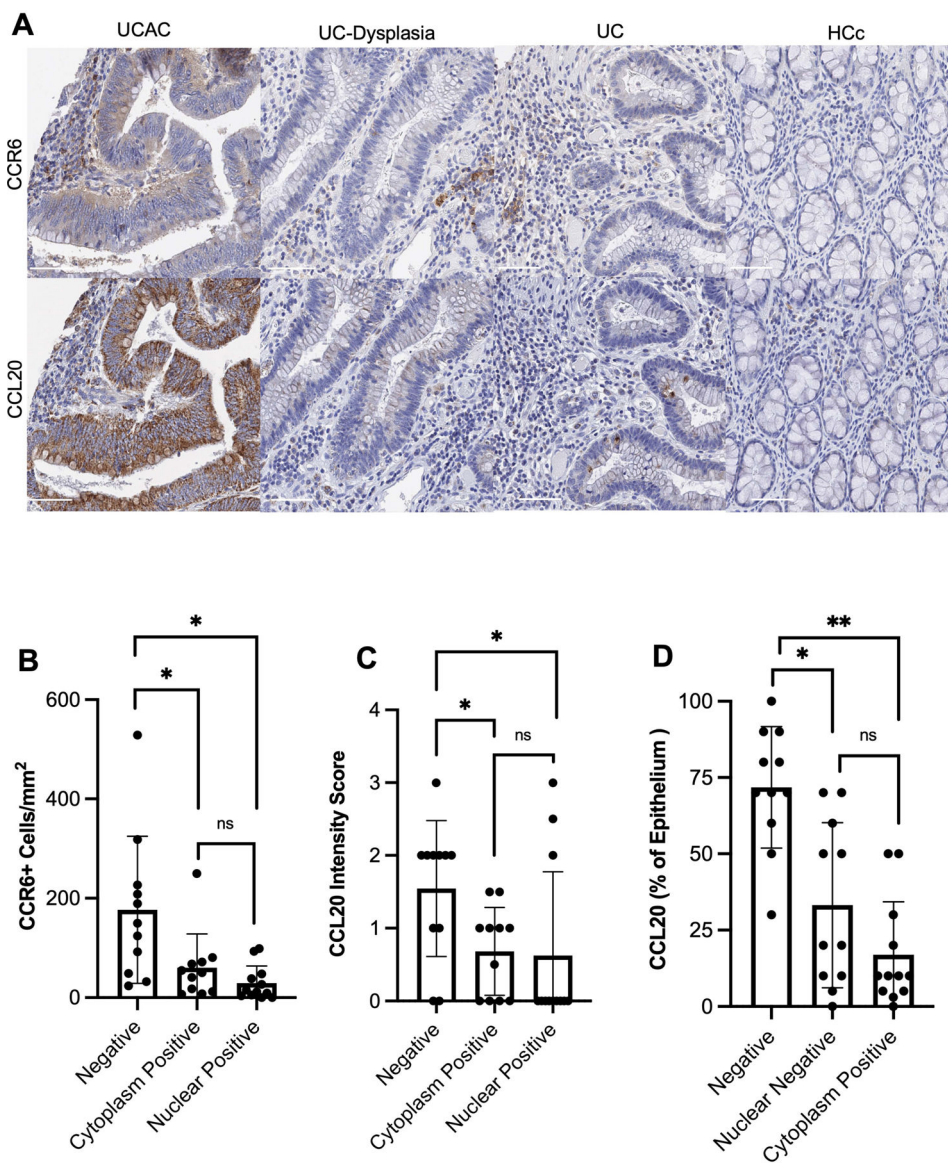


Figure 1. Lack of colon epithelial SMAD4 expression is associated with increased epithelial CCL20 expression and CCR6+ cells.

(A) Representative IHC images of human UCACs (n=34), UC-dysplasia (n=18), UC (n=34), and healthy colon control (n=5) samples for the indicated markers (brown; scale bars: 100µm). (B-D) Quantification according to SMAD4 status indicated on X axis. (B) Quantification of stromal CCR6+ cells/mm², (C) epithelial CCL20 staining score, and (D) CCL20 epithelial percent positivity (data points represent mean per sample if multiple cores exist; Mann-Whitney U test; *P < .05, ** P < .001).

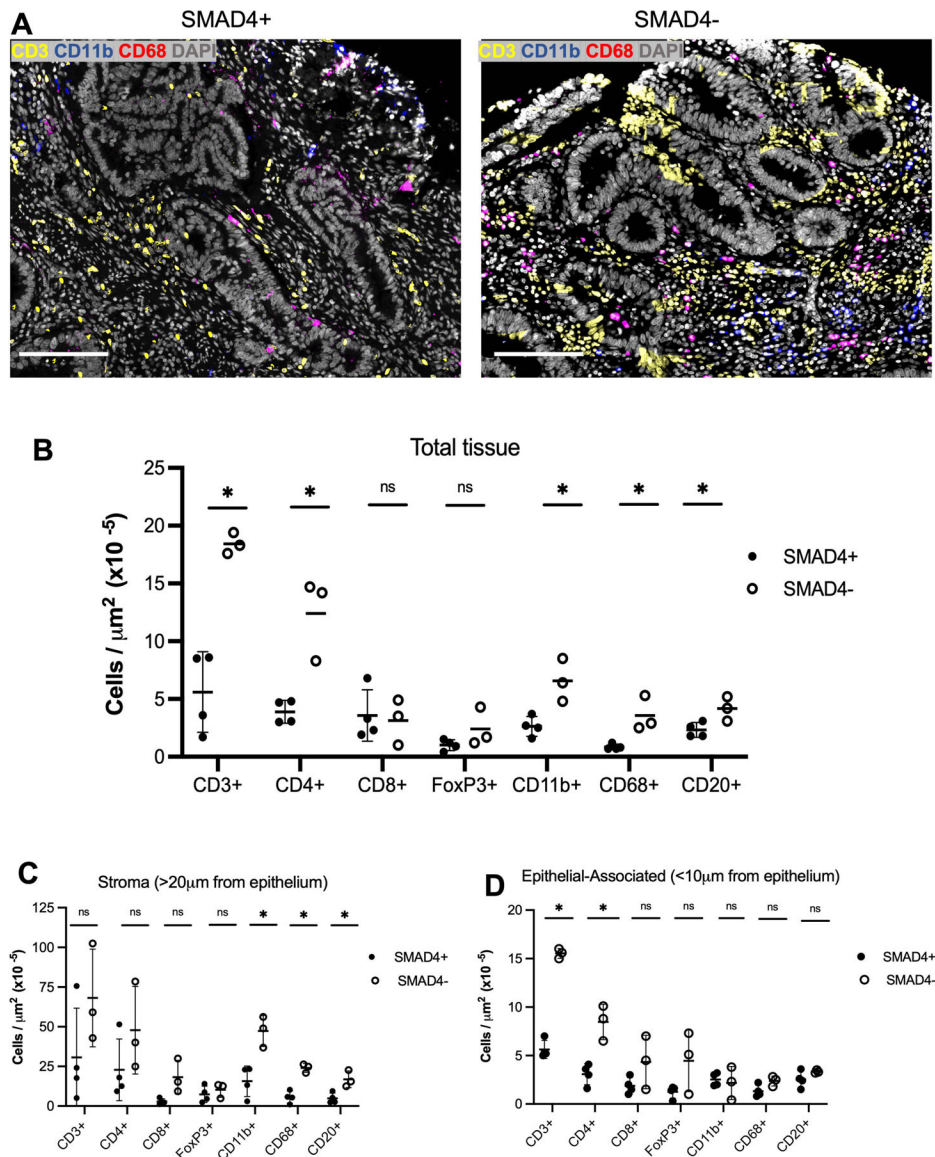


Figure 2. SMAD4 loss is associated with increased immune cell recruitment in human ulcerative colitis-associated cancer specimens.

(A) MxIF of human UCACs (SMAD4+ n=4, SMAD4- n=3) stained for indicated markers

(CD3 = yellow, CD11b = blue, CD68 = red, DAPI = gray; scale bars: 100µm). (B)

Quantification of immune cell types relative to total tissue area. (C) Quantification of

stromal and (D) epithelial-associated immune cells relative to their respective tissue area

(data points represent mean per tumor sample if multiple cores exist; Mann-Whitney *U* test;

P* < .05, *P* < .001).

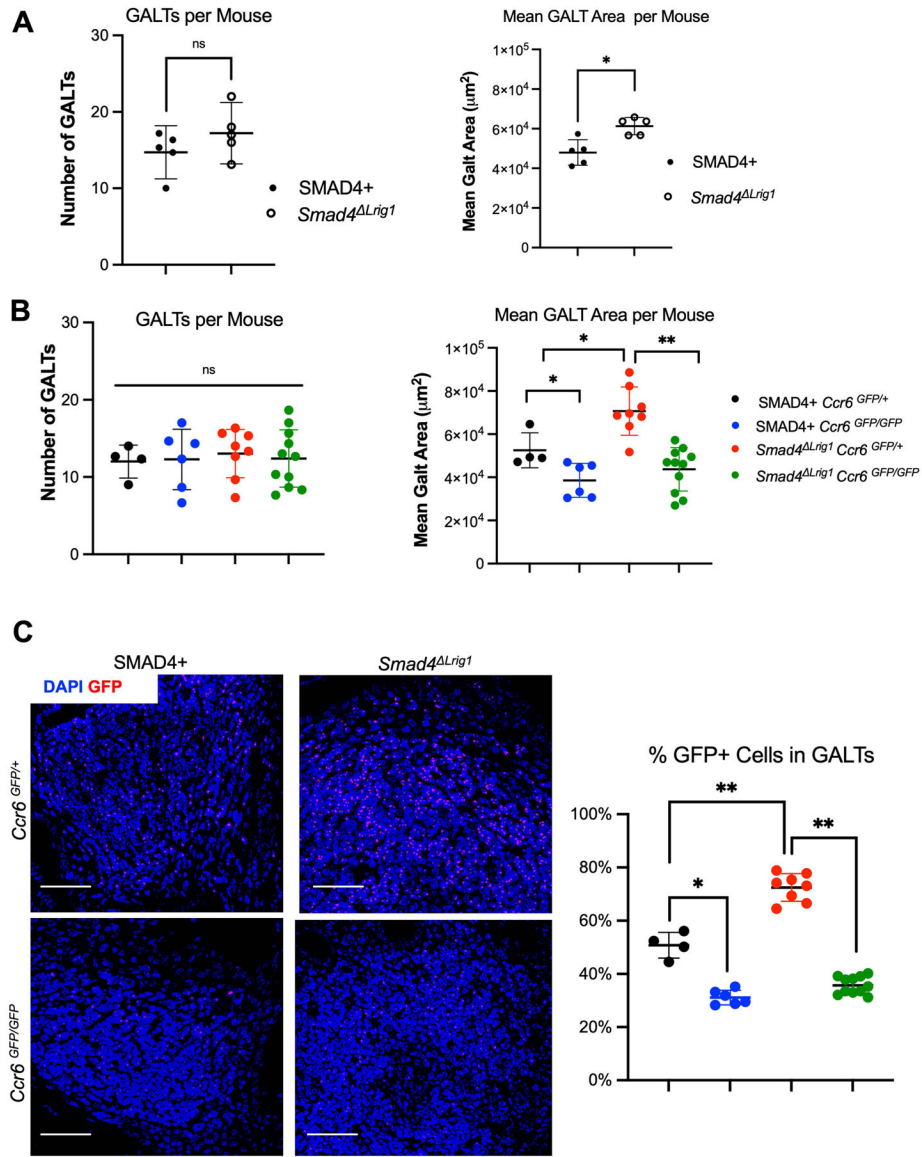


Figure 3. *Smad4* loss results in increased GALT area only when *Ccr6* is expressed. (A) Quantification of GALT number and cross-sectional area from 5 *Smad4*^{Lrig1} and 5 SMAD4+ control mice under homeostatic conditions, (B) and in 4 SMAD4+ *Ccr6*^{GFP/+}, 6 SMAD4+ *Ccr6*^{GFP/GFP}, 8 *Smad4*^{Lrig1} *Ccr6*^{GFP/+}, and 11 *Smad4*^{Lrig1} *Ccr6*^{GFP/GFP} mice, 3 months after completion of DSS-induced colitis. (C) Immunofluorescent staining and quantification for GFP (red) in GALTs from indicated genotypes (Data points represent mean quantification per mouse; DAPI: blue, scale bars: 100μm; Mann-Whitney *U* test; **P* < .05, ** *P* < .001).

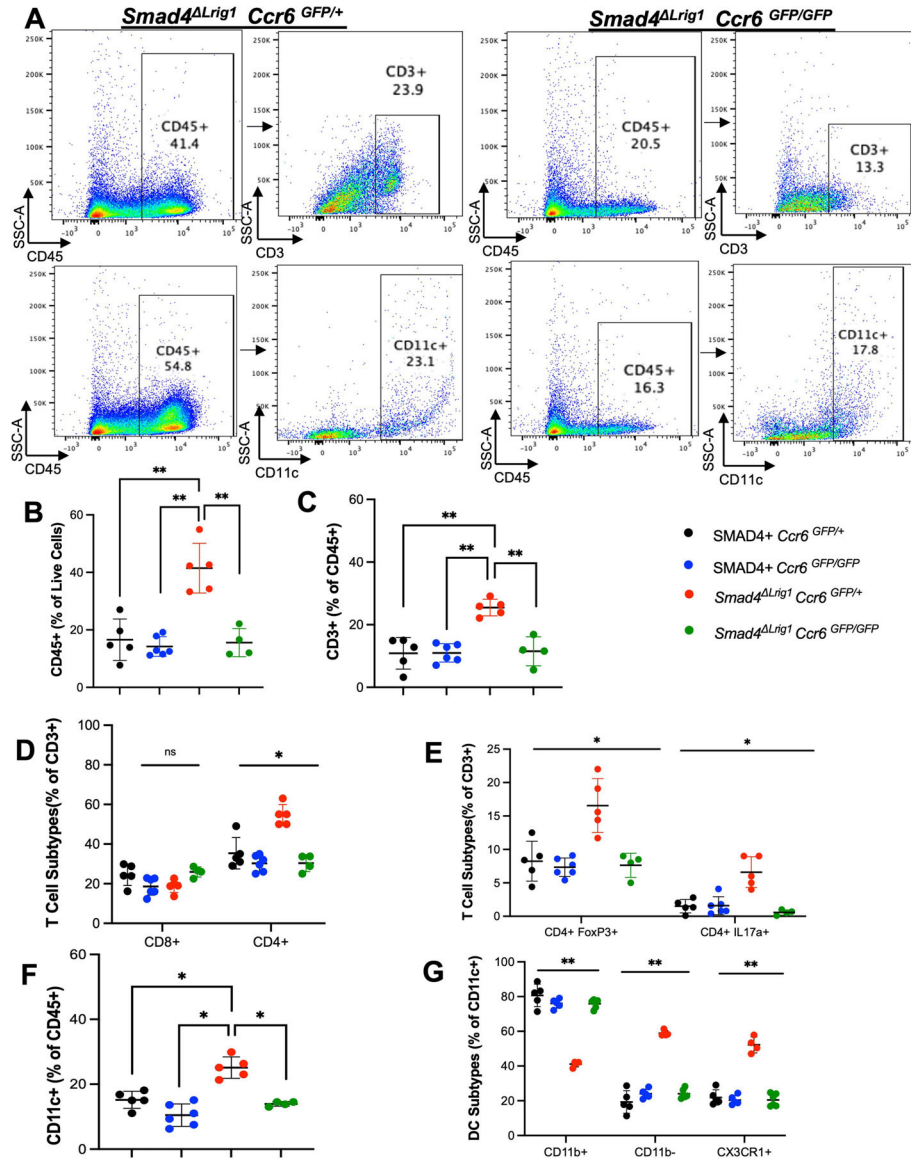


Figure 4. Loss of epithelial *Smad4* results in increased sub-epithelial immune cells in mouse colon in a CCR6-dependent manner.

Colonic stroma from 5 SMAD4+ *Ccr6^{GFP/+}*, 6 SMAD4+ *Ccr6^{GFP/GFP}*, 5 *Smad4^{Lrig1} Ccr6^{GFP/+}*, and 4 *Smad4^{Lrig1} Ccr6^{GFP/GFP}* mice was analyzed by flow cytometry 1 month after completion of DSS-induced colitis. (A) Representative flow cytometry scatter plots showing surface staining of colon stromal CD3+ or CD11c+ in CD45+ cells in a *Smad4^{Lrig1} Ccr6^{GFP/+}* mouse and a *Smad4^{Lrig1} Ccr6^{GFP/GFP}* mouse. Numbers in plot indicate percentage of cells in each gate. (B) Proportion of live stromal cells that were CD45+. (C) Proportion of CD45+ cells that were CD3+. (D) Proportion of CD3+ cells stained for CD8, CD4, (E) CD4 FoxP3, or CD4 IL17a. (F) Proportion of CD45+ cells that were CD11c+. (G) Proportion of CD11c+ cell stained for CD11b or CX3CR1 (Welch's *t* test; **P* < .05, ** *P* < .001).

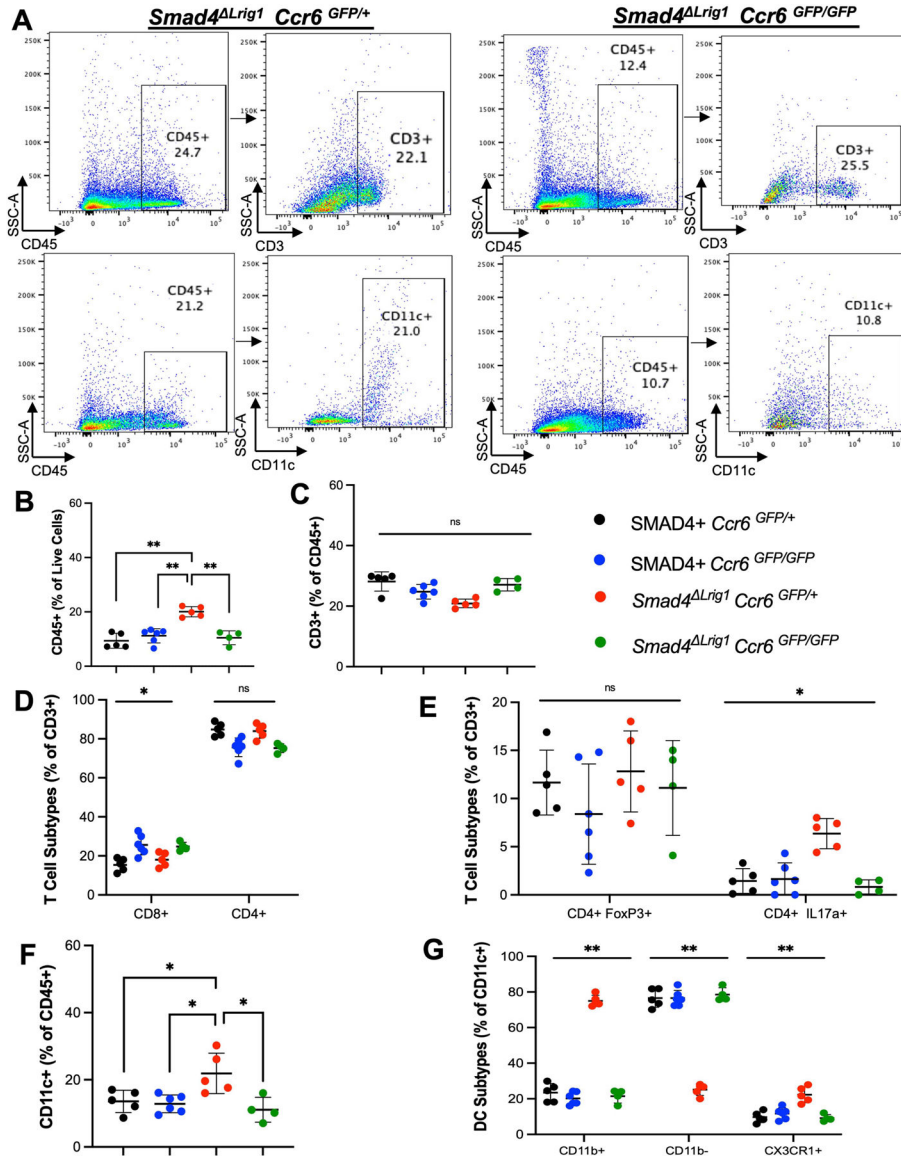


Figure 5. Loss of epithelial *Smad4* results in increased colon epithelial-associated immune cells in a CCR6-dependent manner.

Cells isolated from colonic epithelium of 5 *SMAD4+ Ccr6^{GFP/+}*, 6 *SMAD4+ Ccr6^{GFP/GFP}*, 5 *Smad4^{ΔLrig1} Ccr6^{GFP/+}*, and 4 *Smad4^{ΔLrig1} Ccr6^{GFP/GFP}* mice were analyzed by flow cytometry 1 month after completion of DSS-induced colitis. (A) Representative flow cytometry scatter plots showing surface staining for epithelial-associated CD3+ or CD11c+ in CD45+ cells of a *Smad4^{ΔLrig1} Ccr6^{GFP/+}* mouse and a *Smad4^{ΔLrig1} Ccr6^{GFP/GFP}* mouse. Numbers in plot indicate percentage of cells in each gate. (B) Proportion of live stromal cells that were CD45+. (C) Proportion of CD45+ cells that were CD3+. (D) Proportion of CD3+ cells stained for CD8, CD4, (E) CD4 FoxP3, or CD4 IL17a. (F) Proportion of CD45+ cells that were CD11c+. (G) Proportion of CD11c+ cell stained for CD11b or CX3CR1 (Welch's *t* test; **P* < .05, ***P* < .001).

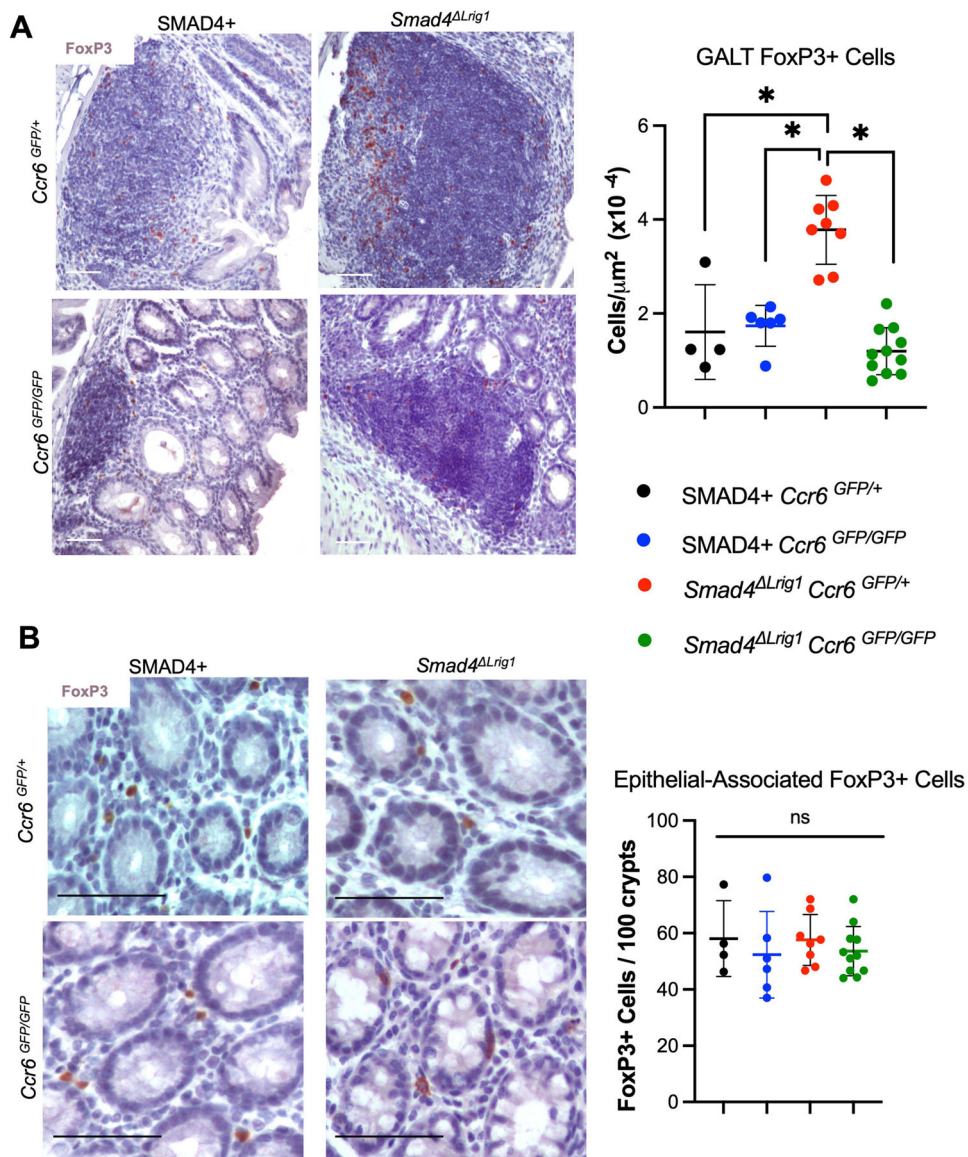


Figure 7. Loss of epithelial *Smad4* resulted in significantly increased FoxP3+ cells in GALTs only in the presence of CCR6.

Staining for FoxP3 (brown) in representative samples for (A) GALTs or (B) crypt-associated regions comparing 4 SMAD4+ *Ccr6^{GFP/+}*, 6 SMAD4+ *Ccr6^{GFP/GFP}*, 8 *Smad4^{Lrig1} Ccr6^{GFP/+}*, and 11 *Smad4^{Lrig1} Ccr6^{GFP/GFP}* mice. (scale bars: 100 μm ; graphs represent quantification of staining; data points represent mean quantification per mouse Mann-Whitney *U* test; **P* < .05).